ELSEVIER

Ceramics International 30 (2004) 9–15

CERAMICS INTERNATIONAL

www.elsevier.com/locate/ceramint

Effect of sintering time on electrical properties and stability against DC accelerated aging of Y_2O_3-doped ZnO-Pr_6O_{11}-based varistor ceramics

Choon-Woo Nahm[a,*], Byoung-Chul Shin[b]

[a]*Department of Electrical Engineering, Dongeui University, Busan 614-714, South Korea*
[b]*Department of Information and Materials Engineering, Dongeui University, Busan 614-714, South Korea*

Received 10 January 2003; received in revised form 3 February 2003; accepted 28 February 2003

Abstract

The electrical nonlinear properties and their stability against DC accelerated aging stress of varistors composed of ZnO–Pr_6O_{11}–CoO–Cr_2O_3–Y_2O_3 (ZPCCY)-based ceramics were investigated at various sintering times. The increase of sintering time deteriorated the nonlinearity, whereas improved the stability. The highest nonlinearity was obtained from the varistor ceramics sintered for 1 h, with 51.2 in nonlinear exponent and 1.3 μA in leakage current. The varistor ceramics sintered for 2 h exhibited not only relatively high nonlinearity, which the nonlinear exponent is 38.6 and the leakage current is 3.9 μA, but also the highest stability, in which the variation rates of varistor voltage, nonlinear exponent, leakage current, and dissipation factor are −0.8%,−1.8%, +74.4%, and +0.9%, respectively, for DC accelerated aging stress such as 0.95 $V_{1\ mA}$/150 °C/12 h.

Keywords: B. Grain boundaries; B. Microstructure; C. Electrical properties; E. Varistors; ZPCCY-based ceramics

1. Introduction

Zinc oxide (ZnO) varistors are semiconducting ceramic devices, produced by sintering ZnO powder containing additives of small amount with varistor former, enhancer, and stabilizer. The voltage–current properties of theses devices exhibited markedly nonlinear properties similar to a pair of back-to-back Zener diode, but with very high-energy absorption capability [1,2]. Therefore, ZnO varistor ceramics are extensively used to protect electrical and electronic systems against dangerous overvoltage surges, such as lightning surges, switching surges, electromagnetic transient surges, and electrostatic discharges.

Nowadays, the electronic components and systems are being became structurally gradually small size and light weight, and functionally multifunction, high frequency, and high reliability. But, as a result, overall insulating strength is being decreased. Therefore, the electronic components and systems are apted to be destructed or they cause malfunction for various surges. In the light of these facts, the high quality varistor ceramics possessing high nonlinearity and stability are required. In particular, the stability of varistor ceramics is very important, because it is directly related to the reliability of systems.

Today, most of commercial ZnO varistors containing Bi_2O_3 as varistor former oxides exhibit excellent varistor properties, but they have a few flaws due to the high volatility and reactivity of Bi_2O_3 having a low melting point [3]. And it is another flaw that Bi_2O_3-based varistors need many additives to obtain the high nonlinearity and stability.

In recent, ZnO–Pr_6O_{11}-based varistor ceramics with another varistor former oxides, Pr_6O_{11}, are actively being researched to overcome a few problems related to Bi_2O_3 [4–17]. One of significant features of these varistor ceramics is a simple microstructure composed of two-phases: ZnO grains and intergranular layers. This gives rise to the increase of effective grain boundary area and ultimately enhances surge-absorption capability.

* Corresponding author.
E-mail address: cwnahm@dongeui.ac.kr (C.-W. Nahm).

0272-8842/03/$30.00
doi:10.1016/S0272-8842(03)00055-5

To apply ZnO–Pr_6O_{11}-based varistor ceramics in various fields, the effect of the experimental variables, such as the kinds and amount of additives, composition ratio, sintering temperature, and cooling rate on the electrical properties and stability of varistor ceramics should be studied. So far, most of the studies on ZnO–Pr_6O_{11}-based varistors have been mainly limited to the ternary system ZnO–Pr_6O_{11}–CoO and further, no their stability has been reported [4–10]. The purpose of this paper is to investigate the effect of sintering time on electrical properties and stability against DC accelerated aging stress of ZnO–Pr_6O_{11}–CoO–Cr_2O_3–Y_2O_3 (ZPCCY)-based varistor ceramics.

2. Experimental procedure

2.1. Sample preparation

Reagent-grade raw materials with composition ratio of (98.0−x) mol% ZnO, 0.5 mol% Pr_6O_{11}, 1.0 mol% CoO, 0.5 mol% Cr_2O_3, x mol% Y_2O_3 (x = 0, 0.5, 1.0, 2.0, 4.0) were used as the starting materials for ZPCCY-based varistor ceramics. Raw materials were mixed by ball milling with zirconia balls and acetone in a polypropylene bottle for 24 h. The mixture was dried at 120 °C for 12 h and calcined in air at 750 °C for 2 h. The calcined mixture was pulverized using an agate mortar/pestle and after 2 wt% polyvinyl alcohol (PVA) binder addition, granulated by sieving 200-mesh screen to produce starting powder. The powder was uniaxially pressed into discs of 10 mm in diameter and 1.8 mm in thickness at a pressure of 800 kg·cm^{-2}. The discs were covered with raw powder in an alumina crucible, sintered at 1350 °C in air for 1–3 h, and furnace-cooled to room temperature. The sintered samples were lapped and polished to 1.0 mm thickness. The size of the final samples was about 8 mm in diameter and 1.0 mm in thickness. Silver paste was coated on both faces of samples and the ohmic contact of electrodes was formed by heating at 600 °C for 10 min. The size of electrodes was 5 mm in diameter.

2.2. Electrical measurement

The voltage–current (V–I) characteristics of ZPCCY-based varistor ceramics were measured by stepping up the linear stair voltage in increment of 0.5 V using a high voltage source-measure unit (Keithley 237). To avoid joule heat of varistors, the varistors were applied up to 50 mA·cm^{-2}. The varistor voltage ($V_{1\ mA}$) was measured at 1.0 mA·cm^{-2} and the leakage current (I_ℓ) was defined as the current at 0.80 $V_{1\ mA}$. In addition, the nonlinear exponent (α) is defined by $\alpha = (\log J_2 - \log J_1)/(\log E_2 - \log E_1)$, where E_1 and E_2 are the electric fields corresponding to J_1 = 1.0 mA·cm^{-2} and J_2 = 10 mA·cm^{-2}, respectively.

The capacitance–voltage (C–V) characteristics of ZPCCY-based varistor ceramics were measured at 1 kHz and 1 V_{rms} using a RLC meter (QuadTech 7600) and a electrometer (Keithley 617). The donor concentration (N_d) of ZnO grains and the barrier height (ϕ_b) at the grain boundary were determined from the slope and intercept of straight line, respectively, using the equation $(1/C_b - 1/2C_{bo})^2 = 2(\phi_b + V_{gb})/q\varepsilon N_d$ proposed by Mukae et al. [18], where C_b is the capacitance per unit area of a grain boundary, C_{bo} is the value of C_b when $V_{gb} = 0$, V_{gb} is the applied voltage per grain boundary, q is the electronic charge, and ε is the permittivity of ZnO ($\varepsilon = 8.5\varepsilon_o$). The density of interface states (N_t) at the grain boundary was determined by the equation $N_t = (2\varepsilon N_d \phi_b/q)^{1/2}$ [18] using the value of the donor concentration and barrier height obtained above. Once the donor concentration and barrier height are known, the depletion layer width (t) of the either side at the grain boundaries was determined by the equation $N_d t = N_t$ [19].

The dielectric characteristics, such as the apparent dielectric constant (ε_{APP}') and dissipation factor (tanδ), were measured in the range of 100 Hz-2 MHz using a RLC meter (QuadTech 7600).

The stability tests were performed under the five continuous DC accelerated aging stress states, such as 0.80 $V_{1\ mA}$/90 °C/12 h in the first stress, 0.85 $V_{1\ mA}$/115 °C/12 h in the second stress, 0.90 $V_{1\ mA}$/120 °C/12 h in the third stress, 0.95 $V_{1\ mA}$/125 °C/12 h in the fourth stress, and 0.95 $V_{1\ mA}$/150 °C/12 h in the fifth stress. Simultaneously, the leakage current during the stress time was monitored at intervals of 1 min by a high voltage source-measure unit (Keithley 237). The varistor ceramics stressed were applied to the electrical characteristics after storage at normal room temperature for 2 h. The degradation rate coefficient (K_T) was calculated from the expression $I_\ell = I_{\ell o} + K_T\ t^{1/2}$, where I_ℓ is the leakage current at stress time (t) and $I_{\ell o}$ is I_ℓ at t = 0 [20]. After the respective stresses, the V−I and dielectric characteristics were measured at room temperature.

2.3. Microstructure measurement

The either surface of samples that the electrical measurement has been finished was lapped and ground with SiC paper and polished with 0.3 μm–Al_2O_3 powder to a mirror-like surface. The polished samples were thermally etched at 1100 °C for 30 min. The surface microstructure was examined by a scanning electron microscope (SEM, Hitachi S2400, Japan). The average grain size (d) was determined by the lineal intercept method, given by $d = 1.56L/MN$, where L is the random line length on the micrograph, M is the magnification of the micrograph, and N is the number of the grain boundaries intercepted by lines [21]. The density (ρ) of varistor ceramics was measured by the Archimedes method.

3. Results and discussion

Fig. 1 shows SEM micrographs of ZPCCY-based varistor ceramics with various sintering times. There are not any phases except for two phases, which are ZnO grains and intergranular layers consisted of Pr- and Y-rich phases regardless of sintering time. The sintered microstructure was more densified with increasing sintering time. The density (ρ) of ceramics was monotonously increased from 5.34 to 5.54 g·cm^{-3} corresponding to 92.39–95.85% of theoretical density (TD = 5.78 g·cm^{-3} in ZnO). It can be seemingly seen from SEM that the pores gradually are decreased with increasing sintering time. The average ZnO grain size (d) was increased in the range of 11.4–15.98 μm as the sintering time increases.

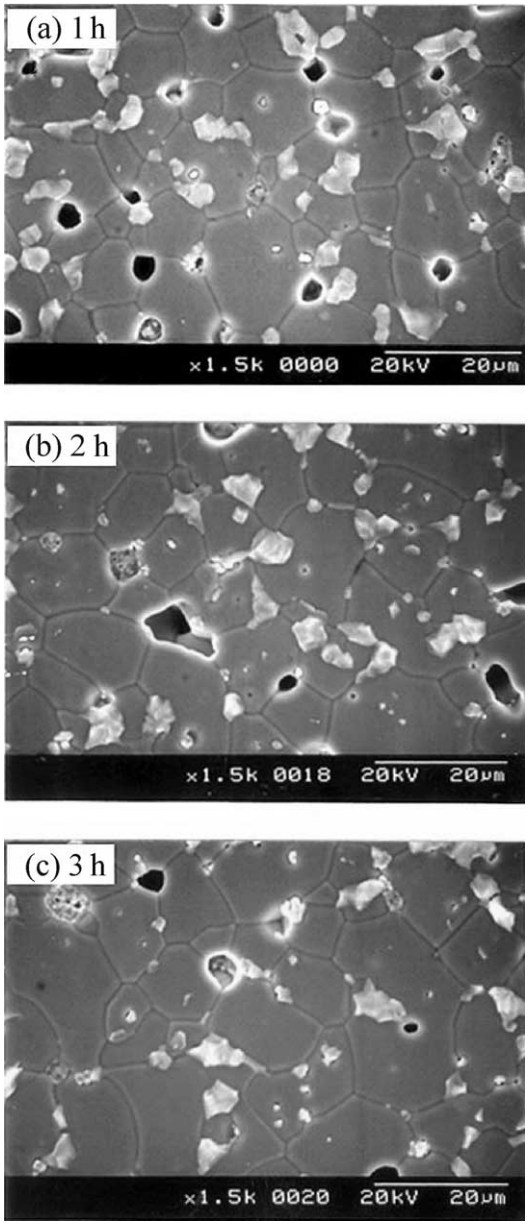

Fig. 1. SEM micrographs of ZPCCY-based varistor ceramics with various sintering times.

Fig. 2 shows the E–J characteristics of ZPCCY-based varistors with various sintering times. The increase of sintering time shifted the E–J curves toward a low electric field and a high current density. It is immediately recognized that this migration of curves will cause a lower nonlinearity. The varistor voltage ($V_{1\ mA}$) was decreased from $V_{1\ mA} = 194.5$ V·mm^{-1} to $V_{1\ mA} = 117.4$ V·mm^{-1} due to the increase of the average grain size with increasing sintering time. The varistor voltage per grain boundaries (V_{gb}), namely, micro-varistor voltage corresponding to breakdown voltage for one junction grain boundary, was in the range of $V_{gb} = 2-3$ V/gb in the varistor ceramics sintered for 1–2 h, whereas the V_{gb} of varistor ceramics sintered for 3 h was comparatively slightly low as $V_{gb} = 1.8$ V/gb. Therefore, it is assumed that the varistor ceramics sintered 3 h exhibit comparatively low nonlinear properties. The nonlinear exponent (α) was decreased linearly from $\alpha = 51.2$ to $\alpha = 23.8$ with increasing sintering time. The α value was found to be relatively high as above $\alpha = 35$ in varistor sintered for 1–2 h, whereas the α value for 3 h was comparatively low. On the other hand, the leakage current (I_ℓ) was increased in the range of from $I_\ell = 1.3$ μA to $I_\ell = 5.6$ μA with increasing sintering time. The tendency of variation in the α value was opposite to that in the I_ℓ value. As a result, it was found that the increase of sintering time deteriorated the nonlinear properties. The variation of V–I characteristic parameters, including the V_{1mA}, V_{gb}, α, and I_ℓ are summarized in Table 1.

Fig. 3 shows the C–V characteristics of ZPCCY-based varistor ceramics with various sintering times. The capacitance decreases due to the increase of depletion layer width at active grain boundaries with increasing DC bias. The modified C–V equation was used to calculate characteristic parameters, such as the donor concentration and barrier height (ϕ_b). The variation of C–V characteristic parameters, including the donor

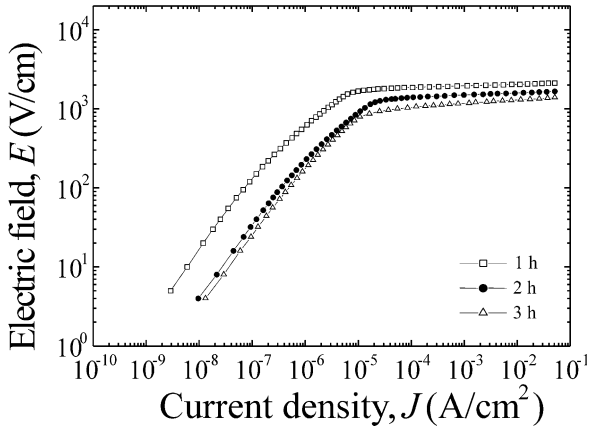

Fig. 2. The E–J characteristics of ZPCCY-based varistor ceramics with various sintering times.

Table 1
The microstructural, *V–I*, *C–V*, and dielectric characteristic parameters of ZPCCY-based varistor ceramics with various sintering times

Sintering time	d (μm)	ρ (g·cm^{-3})	$V_{1\ mA}$ (V·mm^{-1})	V_{gb} (V/gb)	α	I_ℓ (μA)	N_d (10^{18} cm^{-3})	N_t (10^{12} cm^{-2})	Φ_b (eV)	t (nm)	ε_{APP}' (1 kHz)	tanδ (1 kHz)
1 h	11.4	5.34	194.5	2.2	51.2	1.3	1.25	3.64	1.13	29.1	1589.8	0.043
2 h	13.9	5.41	149.3	2.1	38.6	3.9	1.42	3.78	1.07	26.6	2047.3	0.057
3 h	15.9	5.54	117.4	1.9	23.8	5.6	1.73	4.19	1.08	24.1	2485.7	0.062

concentration (N_d), density of interface states (N_t), barrier height (ϕ_b), and depletion layer width (t) is summarized in Table 1.

The N_d was increased in the range of $N_d = 1.25\times10^{18}$–1.73×10^{18} cm^{-3} with increasing sintering time. The increase of N_d with sintering time is assumed to due to decrease of oxygen. The N_d is related to the partial pressure of oxygen (Po_2), namely, $N_d \propto Po_2^{-1/4}$ or $Po_2^{-1/6}$. It is, therefore, believed that the It is assumed that the increase of N_d is attributed to the decrease of the partial pressure of oxygen as the sintering time increases. The t on either side of depletion region was increased in the range of $t = 29.1$–24.1 nm with increasing sintering time. This shows opposite relation to the N_d. In general, the depletion region extends farther into the side with a lighter doping. On the other hand, the increase of sintering time led to the increase the N_t in the range of $N_t = 3.64\times10^{12}$–4.19×10^{12} cm^{-2}. The ϕ_b in the varistor ceramics sintered for 1 h showed maximum value (1.13 eV), whereas the increase of sintering time further fixed ϕ_b to roughly $\phi_b = 1.07$–1.08 eV. The ϕ_b is directly associated with the N_d and N_t. In other words, the ϕ_b is estimated by the variation rate in the N_t and N_d. In general, the ϕ_b is increased with increasing N_t and decreasing N_d. If the variation rate of N_d is much larger than that of N_t with an additive content, the ϕ_b is much more strongly affected by the N_d than the N_t. According to this reason, it can be understood that the ϕ_b is increased or decreased with increasing sintering time.

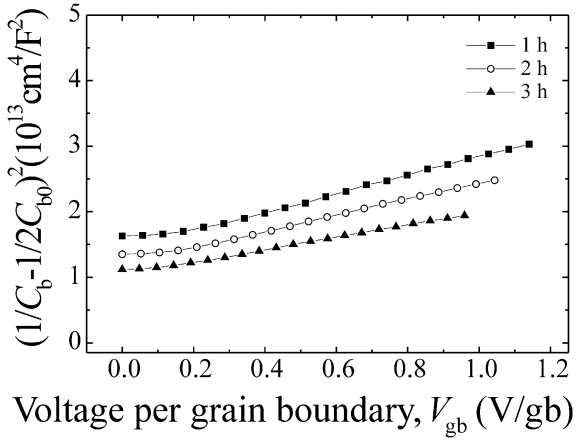

Fig. 3. The *C–V* characteristics of ZPCCY-based varistor ceramics with various sintering times.

Fig. 4 shows the frequency variation of dielectric parameters of ZPCCY-based varistor ceramics with sintering time. The apparent dielectric constant (ε_{APP}') was decreased gradually without a sharper dispersive drop evident as the frequency is increased, which is associated with the polarization of dielectrics. The ε_{APP}' in the measuring frequency range increases with increasing sintering time. This is directly related to the average grain size, as can be seen in the following equation, $\varepsilon_{APP}' = \varepsilon_g(d/t)$, where ε_g is the dielectric constant of ZnO, d is the average grain size, and t is the depletion layer width. That is, this is because the increase of sintering time causes total depletion layer width within entire bulk due to the increase of average grain size. The detailed dielectric parameters, including the apparent dielectric constant (ε_{APP}') and dissipation factor (tanδ) are summarized in Table 1. All curves of tanδ exhibit a similar behavior, whereas a complicated curve, known the dielectric dispersion phenomenon. In

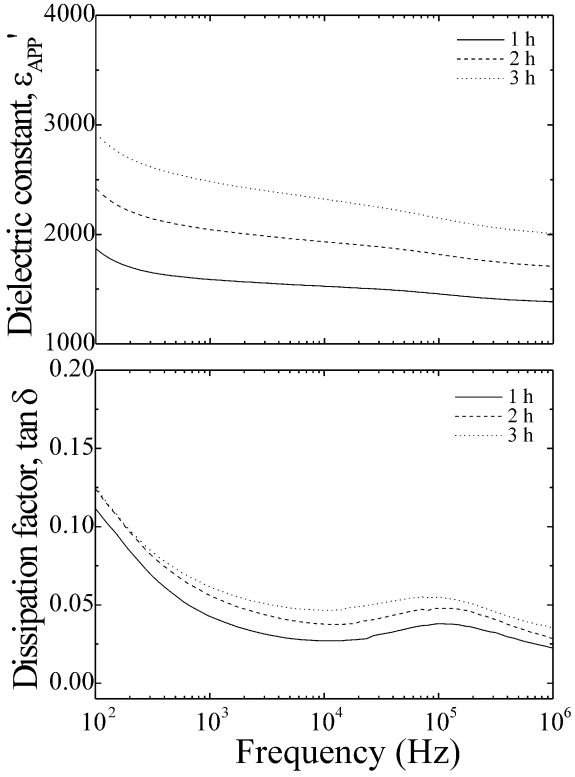

Fig. 4. The dielectric characteristics of ZPCCY-based varistor ceramics with sintering time.

other words, the tanδ is decreased as frequency increase until a minimum is obtained. After a minimum, the tanδ increased to maximum with increasing frequency and thereafter again decreased. It was found that the values of tanδ are not greatly affected by sintering time. The tanδ was increased in the range of tan$\delta = 0.043-0.062$ with increasing sintering time at 1 kHz and is not so high. The increase of the tanδ is assumed to due to the increase of leakage current (I_ℓ).

Abnormal dielectric cannot be seen clearly through ε_{APP}' curve, but it is assumed to be the vicinity of 100 kHz through the peak of tanδ. In general, the abnormal dispersion appears at peak of tanδ.

In practice, ZnO varistors are always subjected to a continuous normal electrical stress, lightning surge, and switching surge. Under such surges, they are gradually degraded with time. Therefore, the high electrical stability against stress is very important in the light of reliability of various electrical and electronic systems. Fig. 5 shows the variation of leakage current of ZPCCY-based varistor ceramics during various DC accelerated aging stresses. On the whole, all ZnO varistor ceramics revealed a good stability. The varistor ceramics exhibited nearly constant leakage current until the third stress, but thereafter the leakage current was increased gradually with stressing time.

The stability of ZnO varistor ceramics against DC accelerated aging stress can be estimated from the degradation rate coefficient (K_T), as indicated in Fig. 6. The K_T value was increased, as DC accelerated aging stress is more severe and increased abruptly after the fourth stress. After the fifth stress, the K_T value was the highest (13.3 $\mu A \cdot h^{-1/2}$) in the varistor ceramics sintered for 1 h and the lowest (3.7 $\mu A \cdot h^{-1/2}$) in the varistor ceramics sintered for 2 h. This suggests the varistor ceramics sintered for 2 h will exhibit the highest stability.

The detailed variation of V–I characteristic parameters after various DC accelerated aging stresses is summarized in Table 2. In an aspect of the stability of V–I characteristics, the variation rate of the varistor voltage ($\%\Delta V_{1\,mA}$) should be lower than any variation rate of parameters. The varistor ceramics sintered for 1 h, after the fifth stress, exhibited low $\%\Delta V_{1\,mA}$ of -1.4% and $\%\Delta\alpha$ of -4.9%, whereas that exhibited high $\%\Delta I_\ell$ of $+507.7\%$. The varistor ceramics sintered for 3 h exhibited the lowest $\%\Delta I_\ell$ of $+5.4\%$, whereas that exhibited the highest $\%\Delta V_{1\,mA} = -2.6\%$. On the other hand, the varistor ceramics sintered for 2 h exhibited very high stability, with $\%\Delta V_{1\,mA}$ of -0.8%, $\%\Delta\alpha$ of -1.8%, and $\%\Delta I_\ell$ of $+74.4\%$. Theses varistor ceramics show that the $\%\Delta I_\ell$ is somewhat high, but the $\%\Delta V_{1\,mA}$ and

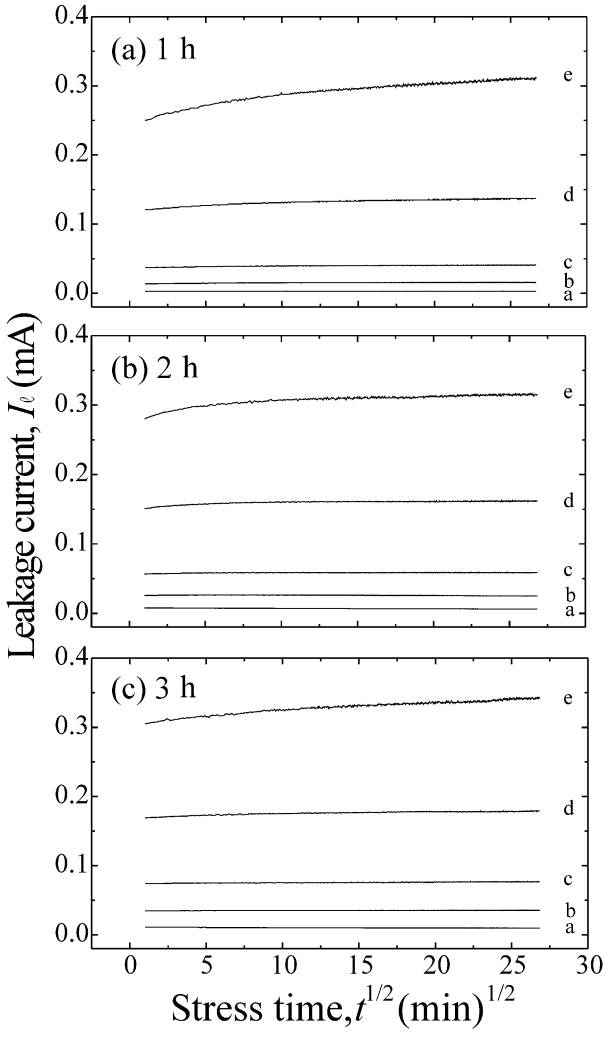

Fig. 5. The variation of leakage current of ZPCCY-based varistor ceramics during various DC accelerated aging stresses with various sintering times; a: the first stress, b: the second stress, c: the third stress, d: the fourth stress, and e: the fifth stress.

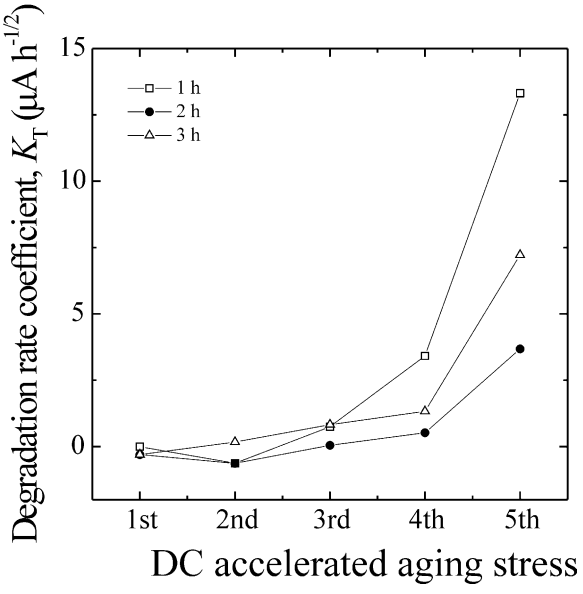

Fig. 6. The degradation rate coefficient (K_T) as a function of DC accelerated aging stress of ZPCCY-based varistor ceramics with various sintering times.

Table 2
The variation of V–I characteristic parameters after various DC accelerated aging stresses of ZPCCY-based varistor ceramics with various sintering times

Sintering time	Stress state	$V_{1\ mA}$ (V·mm^{-1})	$\%\Delta V_{1\ mA}$	α	$\%\Delta\alpha$	I_ℓ (μA)	$\%\Delta I_\ell$
1 h	Before	194.5	0	51.2	0	1.3	0
	1st	194.5	0	51.2	0	1.2	−7.7
	2nd	194.0	−0.3	51.1	−0.2	2.6	100.0
	3rd	193.6	−0.5	50.8	−0.8	2.6	100.0
	4th	193.0	−0.8	50.1	−2.1	3.4	161.5
	5th	191.7	−1.4	48.7	−4.9	7.9	507.7
2 h	Before	149.3	0	38.6	0	3.9	0
	1st	149.2	−0.1	38.5	−0.3	2.2	−43.6
	2nd	149.1	−0.1	38.5	−0.3	2.8	−28.2
	3rd	149.0	−0.2	38.4	−0.5	2.3	−41.0
	4th	148.7	−0.4	36.7	−4.9	2.9	−25.6
	5th	148.1	−0.8	37.9	−1.8	6.8	74.4
3 h	Before	117.4	0	23.8	0	5.6	0
	1st	117.2	−0.2	23.8	0	4.1	−26.8
	2nd	116.9	−0.4	23.6	−0.8	4.4	−21.4
	3rd	116.4	−0.9	23.3	−2.1	4.8	−14.3
	4th	115.9	−1.3	23.0	−3.4	5.2	−7.1
	5th	114.3	−2.6	23.0	−3.4	5.9	5.4

Table 3
The variation of dielectric parameters of ZPCCY-based varistor ceramics after various DC accelerated aging stresses with various sintering times

Sintering time	Stress state	ε_{APP}'	$\%\Delta\varepsilon_{APP}'$	tanδ	% Δtanδ
1 h	Before	1589.8	0	0.043	0
	1st	1523.1	−4.2	0.034	−21.5
	2nd	1588.7	−0.1	0.041	−6.2
	3rd	1590.1	0.0	0.043	−1.6
	4th	1594.2	0.3	0.048	10.6
	5th	1619.7	1.9	0.069	60.1
2 h	Before	2047.3	0	0.057	0
	1st	2039.3	−0.4	0.049	−13.4
	2nd	2119.3	3.4	0.049	−13.0
	3rd	2126.6	3.9	0.049	−14.3
	4th	2130.6	4.1	0.049	−13.7
	5th	2145.5	4.8	0.057	0.9
3 h	Before	2485.7	0	0.062	0
	1st	2588.3	4.1	0.058	−6.3
	2nd	2608.3	4.9	0.060	−4.0
	3rd	2612.0	5.1	0.062	−0.2
	4th	2623.3	5.5	0.066	5.5
	5th	2661.8	7.1	0.068	8.8

$\%\Delta\alpha$ are considerably low, in particular, this varistor exhibited very good stability, compared with other varistor ceramics reported [14–17].

Furthermore, the sintering time greatly affected the stability of dielectric characteristics. The dielectric parameters, such as the variation rate of apparent dielectric constant ($\%\Delta\varepsilon_{APP}'$) and the variation rate of dissipation factor ($\%\Delta\tan\delta$) before and after the stress are summarized in Table 3. After the fifth stress, the varistor ceramics sintered for 1 h exhibited the lowest $\%\Delta\varepsilon_{APP}'$ of +1.9%, whereas the highest $\%\Delta\tan\delta$ of 60.1%. The varistor ceramics sintered for 3 h exhibited the highest $\%\Delta\varepsilon_{APP}'$ of 7.1%. On the contrary, the varistor ceramics sintered for 2 h exhibited the lowest $\%\Delta\tan\delta$ of 0.9%. In the light of these results, it is assumed that the stability of dielectric characteristics is obtained from the varistor ceramics sintered for 2 h.

In discussing stability, the model for stability of varistor ceramics according to various stresses is known to be ion migration mechanism proposed by Gupta and Carlson [22]. The Zn_i is diffused by biasing field and successively reacts with grain boundary defects. As a result, this process leads to a reduction of potential barrier and an increase of leakage current. Therefore, the way to improve the stability is to restrict the generation of Zn_i within depletion layer or the migration of Zn_i toward grain boundaries. It is assumed that the sintering time affects the migration of zinc interstitial (Zn_i) within depletion layer or the stabilization of interface states.

4. Conclusions

The electrical characteristics, and their stability for DC accelerated aging stress of ZPCCY ($\underline{Z}nO$–$\underline{Pr}_6O_{11}$–$\underline{C}oO$–$\underline{Cr}_2O_3$–$\underline{Y}_2O_3$)-based varistor ceramics were investigated at various sintering times. The nonlinear exponent was decreased in the range of 51.2–23.8 and the leakage current was increased in the range of 1.3–5.9 μA as the sintering time increases. The increase of sintering time deteriorated the nonlinear properties, but the proper increase of sintering time was found to improve the stability against DC accelerated aging stress. On the whole, all the varistors exhibited relatively good stability. After the fifth stress, the varistor sintered for 2 h exhibited the highest stability, in which $\%\Delta V_{1\ mA} = -0.8\%$, $\%\Delta\alpha = -1.8\%$, and $\%\Delta I_\ell = +74.4\%$ in the V–I characteristics, and $\%\Delta\varepsilon_{APP}' = +4.8\%$ and $\%\Delta\tan\delta = +0.9\%$ in the dielectric characteristics.

Acknowledgements

This article was financially supported by the Research Center for Electronic Ceramics (RCEC) of Dongeui University founded by the Korea Science and Engineering Foundation (KOSEF), Ministry of Science and Technology (MOST) and the Busan Metropolitan City Government.

References

[1] L.M. Levinson, H.R. Pilipp, Zinc oxide varistor—a review, Am. Ceram. Soc. Bull. 65 (1986) 639–646.

[2] T.K. Gupta, Application of zinc oxide varistor, J. Am. Ceram. Soc. 73 (1990) 1817–1840.

[3] Y.-S. Lee, T.-Y. Tseng, Phase identification and electrical properties in ZnO-glass varistors, J. Am. Ceram. Soc. 75 (1992) 1636–1640.

[4] A.B. Alles, V.L. Burdick, The effect of liquid-phase sintering on the properties of Pr_6O_{11}-based ZnO varistors, J. Appl. Phys. 70 (1991) 6883–6890.

[5] A.B. Alles, R. Puskas, G. Callahan, V.L. Burdick, Compositional effect on the liquid-phase sintering of praseodymium oxides-based ZnO varistors, J. Am. Ceram. Soc. 76 (1993) 2098–2102.

[6] Y.-S. Lee, K.-S. Liao, T.-Y. Tseng, Microstructure and crystal phases of praseodymium in zinc oxides varistor ceramics, J. Am. Ceram. Soc. 79 (1996) 2379–2384.

[7] N. Wakiya, S.Y. Chun, C.H. Lee, O. Sakurai, K. Shinozaki, N. Mizutani, Effect of liquid phase and vaporization on the formation of microstructure of Pr doped ZnO varistor, J. Electroceram. 4:S1 (1999) 15–23.

[8] S.Y. Chun, K. Shinozaki, N. Mizutani, Formation of varistor characteristics by the grain-boundaries penetration of ZnO–PrO_x liquid into ZnO ceramics, J. Am. Ceram. Soc. 82 (1999) 3065–3068.

[9] S.Y. Chun, N. Mizutani, Mass transport via grain boundary in Pr-based ZnO varistors and related electrical effects, Mater. Sci. Eng. B79 (2001) 1–5.

[10] C.-W. Nahm, C.-H. Park, H.-S. Yoon, Microstructure and varistor properties of ZnO–Pr_6O_{11}–CoO–Nd_2O_3 based ceramics, J. Mater. Sci. Lett. 19 (2000) 271–274.

[11] C.-W. Nahm, C.-H. Park, H.-S. Yoon, Highly stable nonohmic characteristics of ZnO–Pr_6O_{11}–CoO–Dy_2O_3 based varistors, J. Mater. Sci. Lett. 19 (2000) 725–728.

[12] C.-W. Nahm, The electrical properties and d.c. degradation characteristics of Dy_2O_3 doped Pr_6O_{11}-based ZnO varistors, J. Eur. Ceram. Soc. 21 (2001) 545–553.

[13] C.-W. Nahm, C.-H. Park, Effect of Er_2O_3 addition on the microstructure, electrical properties, and stability of Pr_6O_{11}-based ZnO ceramic varistors, J. Mater. Sci. 36 (2001) 1671–1677.

[14] C.-W. Nahm, The nonlinear properties and stability of ZnO–Pr_6O_{11}–CoO–Cr_2O_3–Er_2O_3 ceramic varistors, Mater. Lett. 47 (2001) 182–187.

[15] C.-W. Nahm, H.-S. Yoon, J.-S. Ryu, The nonlinear properties and d.c. degradation characteristics of ZPCCE based varistors, J. Mater. Sci. Lett. 20 (2001) 393–395.

[16] C.-W. Nahm, B.-C. Shin, Effect of sintering temperature on electrical properties and stability of Pr_6O_{11}-based ZnO varistors, J. Mater. Sci.: Mater. in Electronic 13 (2002) 111–120.

[17] C.-W. Nahm, ZnO–Pr_6O_{11}–CoO–Cr_2O3–Er_2O_3-based ceramic varistors with high stability of nonlinear properties, J. Mater. Sci. Lett. 21 (2002) 201–204.

[18] M. Mukae, K. Tsuda, I. Nagasawa, Capacitance-vs-voltage characteristics of ZnO varistor, J. Appl. Phys. 50 (1979) 4475–4476.

[19] L. Hozer, Semiconductor Ceramics: Grain Boundary Effects, Ellis Horwood, London, 1999.

[20] J. Fan, R. Freer, Deep level transient spectroscopy of zinc oxide varistors doped with aluminum oxide and/or silver oxide, J. Am. Ceram. Soc. 77 (1994) 2663–2668.

[21] J.C. Wurst, J.A. Nelson, Lineal intercept technique for measuring grain size in two-phase polycrystalline ceramics, J. Am. Ceram. Soc. 55 (1972) 109–111.

[22] T.K. Gupta, W.G. Carlson, A grain boundary defect model for instability/stability of a ZnO varistor, J. Mater. Sci. 20 (1985) 3487–3500.